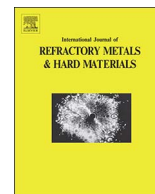




Contents lists available at ScienceDirect

International Journal of Refractory Metals & Hard Materials

journal homepage: www.elsevier.com/locate/IJRMHM

Effects of S on the synthesis of type Ib diamond under high pressure and high temperature

Ning Chen^a, Hongan Ma^{a,*}, Lixue Chen^a, Bingmin Yan^b, Chao Fang^c, Xiaobing Liu^d, Yadong Li^e, Longsuo Guo^a, Liangchao Chen^a, Xiaopeng Jia^{a,*}

HPSTAR
531-2018

^a State Key Laboratory of Superhard Materials, Jilin University, Changchun 130012, China

^b Center for High Pressure Science & Technology Advanced Research (HPSTAR), China

^c School of Physical Engineering, Zhengzhou University, Zhengzhou, Henan 450052, China

^d Department of Earth and Planetary Sciences, Northwestern University, Evanston, IL 60208, USA

^e School of Electrical and Information Engineering, Yangtze Normal University, Chongqing, China

A B S T R A C T

In this study, single crystal diamonds were successfully synthesized in a FeNi-S-C system under the constant conditions of 5.5 GPa and 1400 °C. The growth rate of the diamonds decreased due to the existence of sulfur (S) in the synthesis system. The color of the diamonds changed from yellow to light yellow with an increase in the S content. Compared to common type Ib diamonds synthesized in a FeNi-C system, the nitrogen concentration was higher in the synthesized diamonds when 0.1 wt% S was added but was lower when the amount of S was increased to 0.25 wt%. Raman measurements indicated that the use of S had almost no effect on the diamond lattice structure, thus diamond crystals with a high-quality sp^3 structure were obtained. The photoluminescence (PL) spectra showed that the nitrogen-vacancy (NV) center occurred more likely in diamond lattice growth along the {111} face. Compared to the NV^- center, the NV^0 center could not be easily generated in the type Ib diamond lattice without the addition of S. Even if the NV^0 and NV^- centers were generated simultaneously in the diamond lattice with the addition of 0.25 wt% S, the intensity was higher for the NV^- peak than for the NV^0 peak. The results of this study improve our understanding of the formation mechanisms of natural diamonds and represent an effective method for controlling the NV center in the diamond lattice.

1. Introduction

Diamonds possess excellent physical and chemical properties and are irreplaceable in many fields [1–5]. S is often considered an impurity in natural diamonds and some studies have proposed the hypothesis that natural diamonds may be generated in sulfide melts in the Earth's mantle [6–8]. Recently, researchers found that large gem diamonds were generated from the Fe-Ni-C-S melt in the Earth's deep mantle [9]. Although diamond crystals in S-C, (Fe,Ni)₉S₈-C, FeNi-S-C, and FeNiCo-S-C systems were successfully synthesized, these experiments were carried out by the addition of large amounts of S [6,7] [10–12]. A small amount of S was added to a NiMnCo catalyst using film growth methods (FGM) but the size of the obtained crystals was less than 500 μm [13]. Using a nitrogen getter, the type IIa diamond growth experiment was performed using the temperature gradient growth (TGG) method in a FeNi-S-C system [14]. Although the S content was relatively small in the synthesis system, it had a significant influence on the synthesis and characteristics of the diamonds [13,14]. Nitrogen is the most dominant

impurity in diamonds and both the form and the concentration of the nitrogen atoms have significant effects on most of the physical properties of diamonds. The nitrogen concentration of diamonds synthesized in a (Fe,Ni)₉S₈-C system was estimated at between 850 ppm and 1100 ppm [7], which is considerably higher than the concentration of diamonds grown in a conventional metal-carbon system. In addition, researchers found that the B and H impurities in the synthesis system inhibited the nitrogen atoms entering the diamond structure [15,16]. Similarly, it is unclear whether S in the synthesis system affects the characteristics of the metal catalyst and the nitrogen concentrations in the diamond lattice. Hence, the addition of S to a FeNi catalyst is of great significance in diamond synthesis and in the determination of the formation mechanisms of natural diamonds.

It has been reported that the single nitrogen-vacancy (NV) center represents a promising system for solid-state quantum information processing, nanoscale electromagnetic field sensing, plasmonics, bio-labeling, and other related research fields [17–23]. A common approach for creating the NV center is the irradiation of type Ib diamonds

* Corresponding authors.

E-mail addresses: maha@jlu.edu.cn (H. Ma), jiexp@jlu.edu.cn (X. Jia).

by electrons, protons, neutrons, ions, and gamma photons, this process produces the lattice vacancies that are part of the NV center. Those vacancies are stable until the annealing temperature is in the range of 550–700 °C [24–26]. A single substitutional nitrogen atom will produce strain in the diamond lattice [27], as a result, it is more likely that the moving vacancies are captured when the temperature up the vacancies instability condition [28]. Another method for creating NV center in high purity type IIa CVD diamond is used the high energy N ions implantation and then take the high temperature or high pressure and high temperature (HPHT) treated for combine the N and vacancy. According to the two processes above, NV centers are produced in diamond lattice. Previous studies have not placed much emphasis on the effect of additives in the synthesis system for generating the NV center in a diamond lattice. Our previous research results indicated that an appropriate amount of S was beneficial for the generation of NV⁰ or NV⁻ centers in the type IIa diamond lattice [14]. However, the effects of S, N and the original growth faces for generating NV center in diamond lattice are not clear. Therefore, the introduction of S into a FeNi system for the synthesis of type Ib diamonds requires in-depth research. In this study, synthesized diamonds in FeNi-S-C systems are studied. This research is useful for understanding the genesis of large *gem* natural diamonds and provides a new method for creating the NV center in a diamond lattice.

2. Experimental details

The high pressure and high temperature (HPHT) experiments were carried out using a Chinese SPD-6 × 1200 cubic-anvil high-pressure apparatus (CHPA). The sample assembly (Fig. 1) was used for the diamond synthesis. The raw materials consisted of high purity graphite slices (99.9% purity) as a carbon source, Fe₆₄Ni₃₆ (64/36, weight ratio) alloy as a catalyst, and sulfur powder (99.999% purity) as an additive. The raw materials and the sample assembly were kept in the drying oven to decrease the influence of residual water for the diamond synthesis. Diamond seeds synthesized by the FGM with {100} or {111} crystal faces of 0.7 mm in size were used as the diamond growth faces. The synthetic pressure and temperature were 5.5 GPa and 1400 °C, respectively. The pressure was calibrated by the pressure-induced phase transitions of Bi, Tl, and Ba. In each experiment, a Pt-30% Rh/Pt-6% Rh thermocouple was placed near the crystallization sample to measure the temperature.

After the HPHT experiments, the samples were treated with hot dilute HNO₃ to separate the diamond crystals from the catalyst alloy medium. After the HNO₃ treatment, the diamond crystals were placed in a boiling mixture of H₂SO₄ and HNO₃ to remove the remaining graphite and metal on the crystal surfaces. Prior to the tests, we repeatedly used supersonic wave equipment and deionized water for removing the residual impurities on the diamonds' surfaces. The optical

Table 1
Experimental results of diamond synthesis in the FeNi-S-C system at 5.5 GPa and 1400 °C.

Run	Additive (wt%) S	Growth face	Growth Rate mg/h	Morphology	Color
E-1	0	{100}	0.280	Cub-Octahedron	Yellow
E-2	0.1	{100}	0.157	Cub-Octahedron	Yellow
E-3	0.25	{100}	0.070	Octahedron	Light Yellow
E-4	0	{111}	0.186	Cub-Octahedron	Yellow
E-5	0.1	{111}	0.153	Cub-Octahedron	Yellow
E-6	0.25	{111}	0.062	Octahedron	Light Yellow

microscope (OM) and scanning electron microscope (SEM) were used to observe the morphology of the crystals. The infrared absorption spectra were measured by a Vertex80V Fourier-transform infrared (FTIR) spectrometer with a spectral range between 400 cm⁻¹ and 4000 cm⁻¹ and a spectral resolution of 2 cm⁻¹ in the transmittance mode. The Raman measurements were performed using a spectrometer (iHR550, Horiba Jobin Yvon) with a diode laser at 671 nm (80 cm⁻¹–3500 cm⁻¹) as the excitation source. The laser output power of the samples was maintained at 10 mW. All Raman spectra were collected using a backscattering configuration and the acquisition time for each spectrum was 60 s. The Raman signals were recorded using a liquid nitrogen cooled CCD camera (Symphont II, Horiba Jobin Yvon) with a spectral resolution set at 1 cm⁻¹. The photoluminescence (PL) spectra were measured at 488 nm excitation at room temperature.

3. Results and discussions

The diamond crystal synthesis experiments in the FeNi-S-C system were carried out under a constant condition of 5.5 GPa and 1400 °C, as summarized in Table 1. Diamonds were synthesized in six experimental runs using seed diamonds, runs E-1 to E-3 growth by the {100} faces and runs E-4 to E-6 growth by the {111} faces. After separating the diamond crystals from the metal-catalyst medium, the OM was used to observe the morphology of the crystals. Fig. 2 shows the OM images of the synthesized diamond crystals. Without adding S to the synthesis system, all diamonds exhibit a yellow color and a cub-octahedron shape. When 0.1 wt% S (E-2 and E-4) is added to the FeNi-C system, the color and shape (Fig. 2b) of the diamonds are the same as in the E-1 experiments. When 0.25 wt% S is added to the FeNi-C system, the color of the diamonds changes to light yellow and the shape changes from a cub-octahedron to an octahedron (Fig. 2c and Fig. 2f). The growth rates of the diamonds in the E-1 to E-6 experiments are 0.280 mg/h, 0.157 mg/h, 0.070 mg/h, 0.186 mg/h, 0.153 mg/h, and 0.062 mg/h, respectively. The growth rate is clearly reduced by increasing the S content.

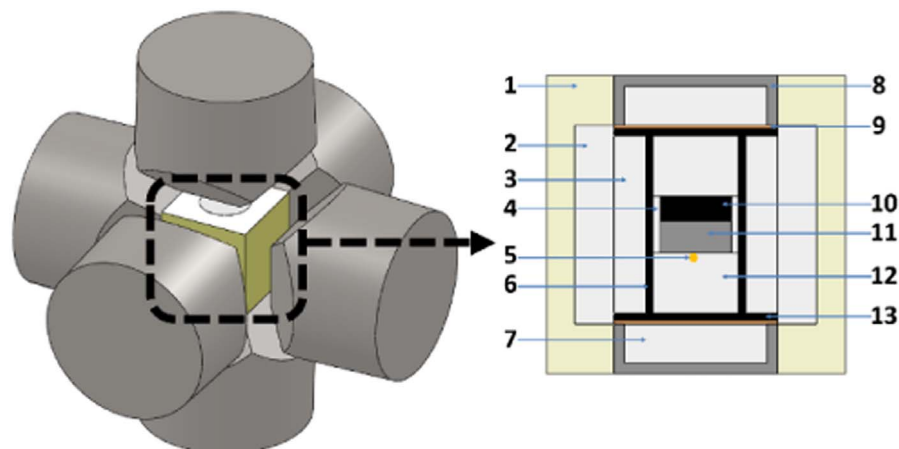


Fig. 1. Sample assembly of the diamond synthesis by HPHT: 1. pyrophyllite; 2. dolomite sleeve; 3. NaCl + ZrO₂ sleeve; 4. ZrO₂ + MgO sleeve; 5. seed crystal; 6. graphite heater; 7. dolomite pillar; 8. steel cap; 9. sheet Cu; 10. carbon source; 11. metal catalyst; 12. ZrO₂ + MgO pillar; 13. sheet graphite.

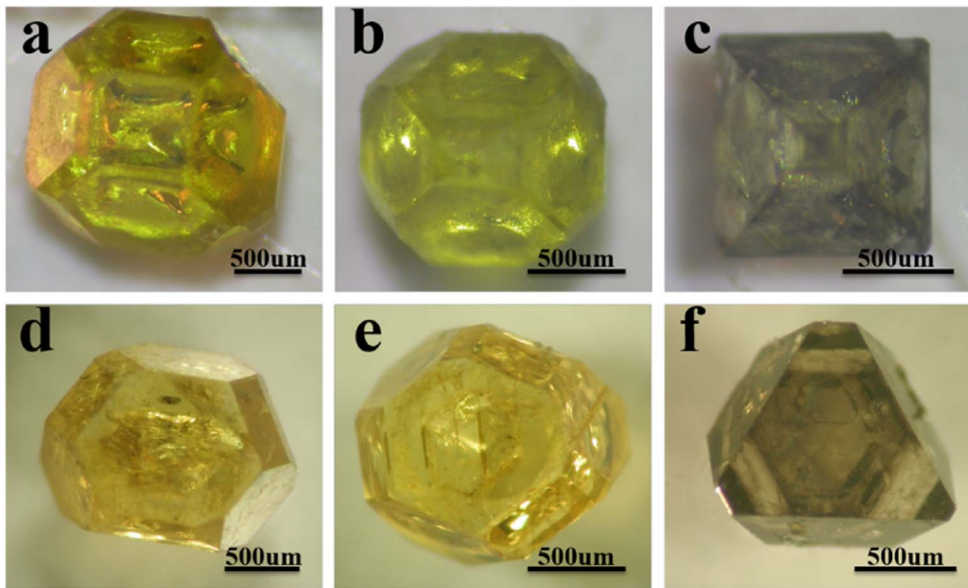


Fig. 2. OM images of the synthetic diamonds created in the FeNi-S-C system; (a), (b), (c), (d), (e), and (f) are obtained in the E-1, E-2, E-3, E-4, E-5, and E-6 experiments, respectively.

The SEM micrographs were used to further analyze the surface characteristics of the synthesized diamond crystals. The SEM micrographs of the synthesized diamonds obtained in the E-1 to E-3 experiments are displayed in Fig. 3. There are no obvious defects on the diamond surfaces as is evident in Fig. 3a and Fig. 3d. The {100} and {111} faces are the main types of crystal surfaces. The micrographs of the diamonds synthesized with 0.1 wt% S are shown in Fig. 3b and Fig. 3e. The diamonds still primarily have {100} and {111} faces but the area is larger for the {111} faces than for the {100} faces and the area of the {113} faces is greater than for the diamond shown in Fig. 3a. Some defects, such as veins or branches appear at the edges of the diamonds. Fig. 3c and Fig. 3f show some irregular defects on the surface of the diamond crystal resulting from the addition of 0.25 wt% S to the synthesis system. The area of the {111} faces is far greater than the area of the {100} faces. Let us now consider the morphological features of the diamond growth along the {111} faces of the seed diamond. Fig. 4a and Fig. 4d show that the synthesized diamonds in the FeNi-S-C system have predominantly {100} and {111} faces and that the surfaces are flat and smooth. The addition of 0.1 wt% S to the synthesis system results in defects such as craters at the edges of the diamonds surfaces. The {100} and {111} faces represent the main type of crystal surface. When S is increased to 0.25 wt%, the edge of the {111} faces of the diamond crystal exhibits some irregular defects as shown in Fig. 3c and Fig. 3f. In addition, diamonds with only {111} faces and {100} faces are not synthesized. Based on the results of the E-1 to E-6 experiments, the

growth of {100} faces are promoted when 0.25 wt% S is introduced to the synthesis system. Otherwise, the growth of the {111} faces is inhibited.

We should note that the growth rate of both synthesized diamonds decreases when S is added to the synthesis chamber. The possible reason is discussed below. In fact, the growth rate of the diamond crystals is largely related to the solubility of carbon in the catalyst alloy. A certain quantity of melted alloy will dissolve fixed carbon under constant HPHT conditions. S has a low magnitude solubility of carbon compared with FeNi alloy, therefore the solubility will decrease when S is dissolved in a saturated melted alloy [29]. Our study is focused on the diamond growth habit using the TGG method under HPHT at a constant condition, which provides the amount of carbon from the heat source to the diamond surface in an amount per unit of time. Importantly, this amount only depends on the solubility of the catalyst solvent. If this theory is applied to diamond crystallization, it can nicely explain the decrease in the diamond growth rate after S was added to the synthesis system.

The FTIR technique is generally utilized to observe the molecular structure to determine the chemical composition and forms of impurity. The crystals are measured with a FTIR spectrometer to determine the spectroscopic details of the synthesized diamonds. Nitrogen is the most common impurity and is easily accessible in the diamond lattice in both natural and synthetic diamonds. Fig. 5 shows that the single substitutional nitrogen atom impurity of the C-center has absorption peaks at

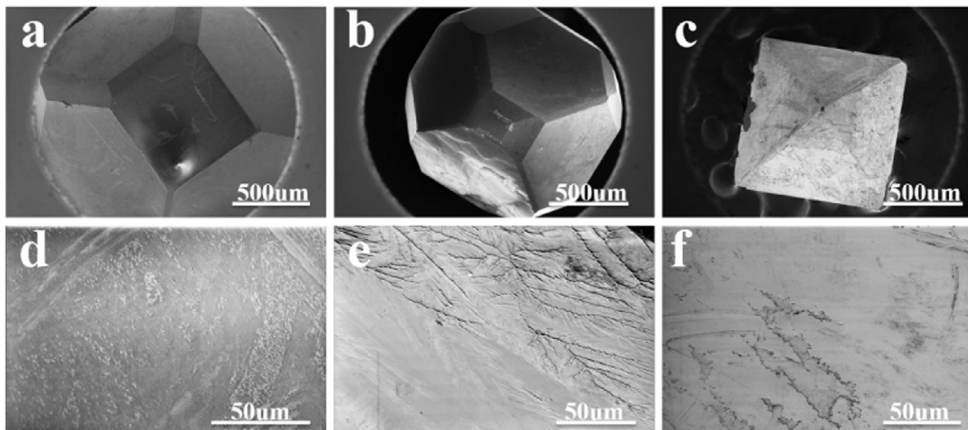


Fig. 3. SEM micrographs of the diamond crystal growth along the {100} face in the FeNi-S-C system; (a), (b), and (c) are obtained in the E-1, E-2, and E-3 experiments; (d), (e), and (f) are the enlarged images of (a), (b), and (c), respectively.

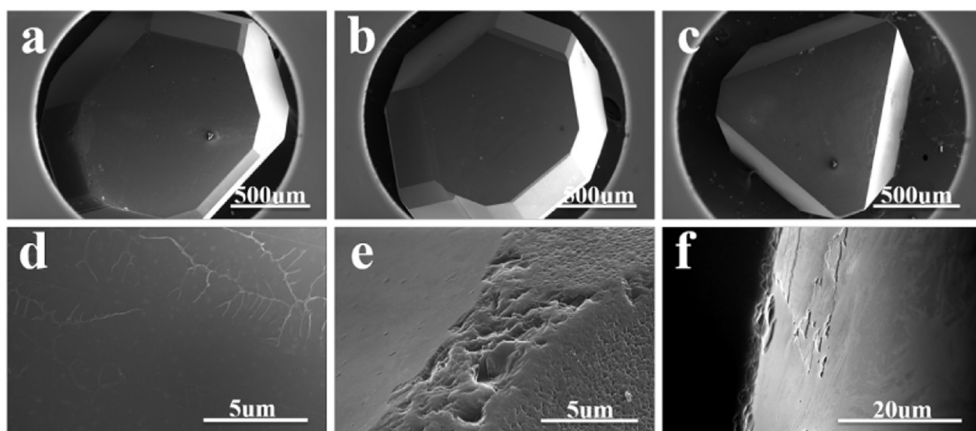


Fig. 4. SEM micrographs of the diamond crystal growth along the {100} face in the FeNi-S-C system; (a), (b), and (c) are obtained in the E-4, E-5, and E-6 experiments; (d), (e), and (f) are the enlarged images of (a), (b), and (c), respectively.

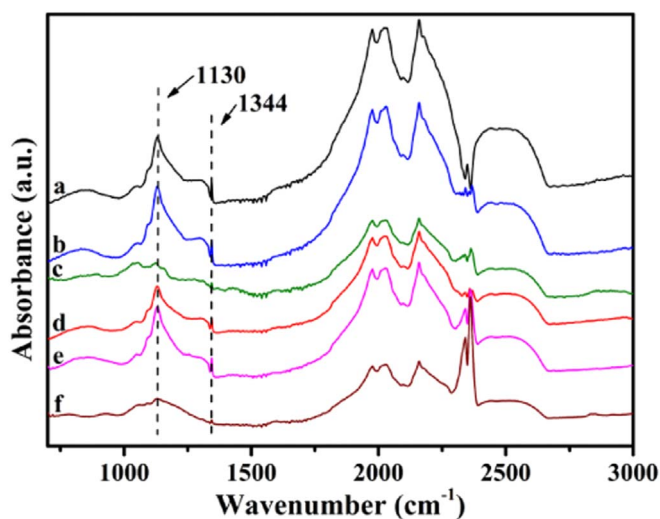


Fig. 5. Infrared absorption spectra for diamond crystals synthesized in the FeNi-S-C system; (a), (b), (c), (d), (e) and (f) are obtained in the E-1, E-2, E-3, E-4, E-5 and E-6 experiment, respectively.

1130 cm^{-1} and 1344 cm^{-1} . A-centers nitrogen that the pairs of nearest neighboring pairs substitutional nitrogen atoms at 1282 cm^{-1} is undetected. Therefore, the one-phonon defect-induced absorption is dominated by a band of C-center nitrogen. The infrared absorption spectra can be used to determine the nitrogen impurity concentration by the following formula [30–32]:

$$N_{\text{C}}(\text{ppm}) = \mu(1130\text{ cm}^{-1})/\mu(1210\text{ cm}^{-1}) \times 5.5 \times 25$$

$$\mu(1130\text{ cm}^{-1}) = [A(1290\text{ cm}^{-1}) - A(1370\text{ cm}^{-1})/0.31]$$

$$\mu(1210\text{ cm}^{-1}) = [(40 \times A(2030\text{ cm}^{-1}) + 87 \times A(2160\text{ cm}^{-1}))]/127 - A(2120\text{ cm}^{-1})]$$

where $N_{\text{C}}(\text{ppm})$ is the concentration of nitrogen, μ and A are the corrected coefficients and the absorption intensity of the relevant peak in the FTIR spectra, respectively. As follows from the infrared absorption measurements, the calculated nitrogen concentrations of the synthesized diamond crystals are summarized in Table 2. The concentrations of nitrogen in the E-1, E-2, E-3, E-4, E-5, and E-6 experiments are 151 ppm, 201 ppm, 144 ppm, 180 ppm, 230 ppm, and 154 ppm, respectively. When 0.1 wt% S is added to the synthesis system, the nitrogen concentrations increase to 201 ppm and 230 ppm in the E-2 and E-4 experiments, respectively. This result is consistent with previous reports of diamonds synthesized in the (Fe,Ni)₃S-C system. Of particular interest is that the concentration of nitrogen decreases to 144 ppm

Table 2

Concentrations of nitrogen impurities in diamonds synthesized in the FeNi-S-C system.

Run	Additive (wt%) S	Nitrogen content (ppm) C-form
E-1	0	151
E-2	0.1	201
E-3	0.25	144
E-4	0	180
E-5	0.1	230
E-6	0.25	154

and 154 ppm in the E-3 and E-4 experiments, respectively when 0.25 wt % S is added to the synthesis system. The changes in nitrogen content may be due to the properties of the FeNi catalyst. When S is added to the synthesis system, the ability of the catalyst alloy to dissolve nitrogen and the mobility of the molten state catalyst change. The S in the synthesis system also affects the formation of C–N bond in another manner. The nitrogen content of the synthesized diamonds largely depends on the properties of the catalyst alloy and ability to form C–N bonds. These topics require more in-depth interpretation and are worthy of further investigation.

Raman spectroscopy is used to identify sp^3 bonding in diamonds from sp^2 in graphite and other inclusions [33]. The Raman peaks of the E-1 to E-6 experiments are shown in Fig. 6. The Raman peaks of the E-1 to E-6 experiments are located at 1330.72 cm^{-1} , 1330.65 cm^{-1} , 1330.43 cm^{-1} , 1330.65 cm^{-1} , 1330.57 cm^{-1} , and 1330.46 cm^{-1} , respectively. It is well known that this represents the typical diamond Raman peaks and no additional peaks were observed, which indicates that all synthesized diamond crystals have a single sp^3 structure. The existence of impurities or inclusions in diamonds will generate residual stresses that cause changes in the C–C bond length, which is reflected by changes in the peak positions in Raman spectra analysis. Fig. 6 shows that the Raman peaks of E-1 to E-3 shift from 1330.72 cm^{-1} to 1330.43 cm^{-1} and E-4 to E-6 shift from 1330.65 cm^{-1} to 1330.46 cm^{-1} after S is added to synthesis system. The data accuracy derived from the Raman spectroscopy is about 1 cm^{-1} . So, added S to diamond synthesis system was not obvious changed the diamond structure. All the Raman spectra exhibit only a very strong and narrow peak with a linear background, which indicates that all the obtained diamond crystals possess a high-quality sp^3 structure [34].

PL was employed to investigate the types of impurities and defects in the synthesized diamond. Fig. 7 shows the PL spectra of the diamond crystals in the FeNi-S-C system in the E-1 to E-6 runs, the right spectrogram is an enlargement of the original spectrum in the indicated region. In Fig. 7, lines a to c are the PL spectra of the diamond growth by {100} faces in the FeNi-S-C system. Line a show the PL spectra without the added S, the NV center is absent in the diamond lattice. Line b exhibits a weak peak PL zero-phonon line at 637 nm due to the

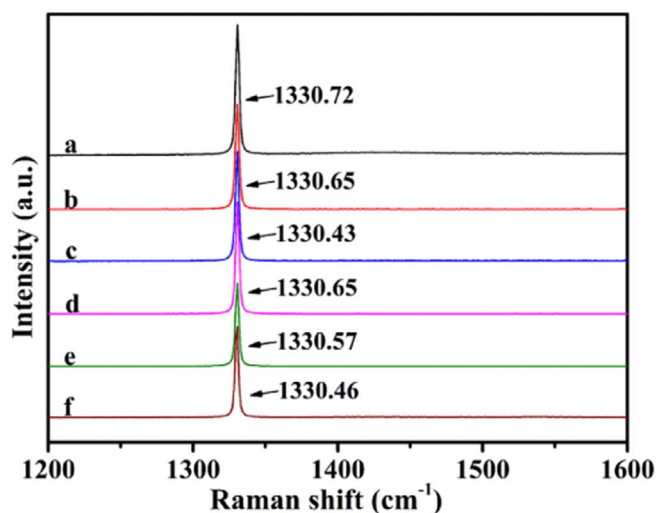


Fig. 6. Raman spectra for diamond crystals synthesized in the FeNi-S-C system. (a), (b), (c), (d), (e) and (f) are obtained in E-1, E-2, E-3, E-4, E-5 and E-6 experiments, respectively.

negatively charged states of the NV^- center [35,36]. Line c exhibits a weak peak at 575 nm due to the neutral charge states and an intense peak appears at 637 nm [35,36]. Lines d to f belong to the diamonds with the $\{111\}$ growth faces. Without added S, a weak peak located at 637 nm is observed in line d. The negligible peaks at 575 nm and 637 nm are observed in diamonds synthesized with 0.1 wt% S (line e). In line f, two intense peaks at 575 nm and 637 nm are observed in the PL spectra. The PL measurements demonstrate that the NV center can be generated easily from the type Ib diamond growth with $\{111\}$ faces in the FeNi-S-C system. In addition, under the same experimental conditions, the intensity is much higher for the 637 nm peak than for the 575 nm peak. This result is different from our previous research on type IIa diamonds, in which the intensity was much higher for the 575 nm peak than for the 637 nm peak when 0.25 wt% S was added to the synthesis system [14].

Fig. 8 shows the schematic diagram of a possible process for the generation of the NV center from the $\{100\}$ crystal orientation when S is added to the synthesis system. The diamond crystallization and growth in this FeNi-S-C environment was more likely to generate vacancies (Fig. 8a) in the diamond lattice than in the common FeNi-C environment. The experiment temperature of 1400 °C was considerably higher than the temperatures of 550–700 °C for the vacancy-stabilized phase [24–26]. The high temperatures provided sufficient kinetic energy for moving the lattice vacancies. In addition, the single substitutional nitrogen atom will produce strain in the diamond lattice,

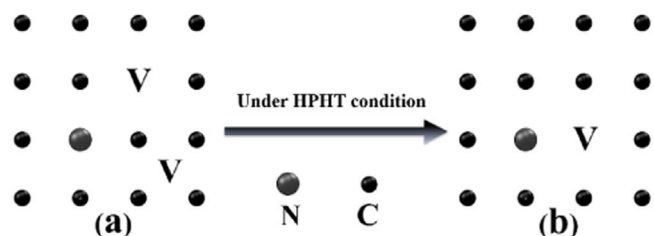


Fig. 8. Schematic of a possible process describing the generation of the NV center from the $\{100\}$ crystal orientation.

therefore the moving vacancies are more likely to be captured [28] and then produce the NV center (Fig. 8b). In addition, high pressure can accelerate this process. Thus, deliberately adjusting the S content to the synthesis system and choosing the seed growth face and the type of synthesized diamonds under HPHT conditions provide an effective and direct method for producing the NV center in the diamond lattice.

4. Conclusions

Diamond synthesis in a FeNi-S-C system was carried out at the constant conditions of 5.5 GPa and 1400 °C. When S is added to the FeNi-S-C system, the color of the diamonds changes from yellow to light yellow and the shape changes from a cub-octahedron to an octahedron. When 0.25 wt% S is added to the synthesis system, the growth of $\{100\}$ faces is promoted and the growth of $\{111\}$ faces is inhibited. When 0.1 wt% S is introduced into the synthesis system, the concentration of nitrogen in the diamond lattice is higher than for a common type Ib diamond. However, the concentration of nitrogen is lower than for a common type Ib diamond when the S content is further increased to 0.25 wt%. The Raman spectra demonstrate that the synthesized diamonds possess a high-quality sp^3 diamond structure. The NV center can be generated easily in the diamond with the $\{111\}$ growth faces under the same experimental conditions. The NV^0 center is more likely to appear when 0.25 wt% is added to the synthesis system. Diamonds obtained from the FeNi-S-C system without a nitrogen getter exhibit a higher intensity for the NV^- center than for the NV^0 center under the same experimental conditions.

Acknowledgements

This work was supported by the National Natural Science Foundation of China (Grant No. 51772120, 51172089, 11604246), Natural Science Foundation of Heilongjiang Province of China (Grant No. QC2017064).

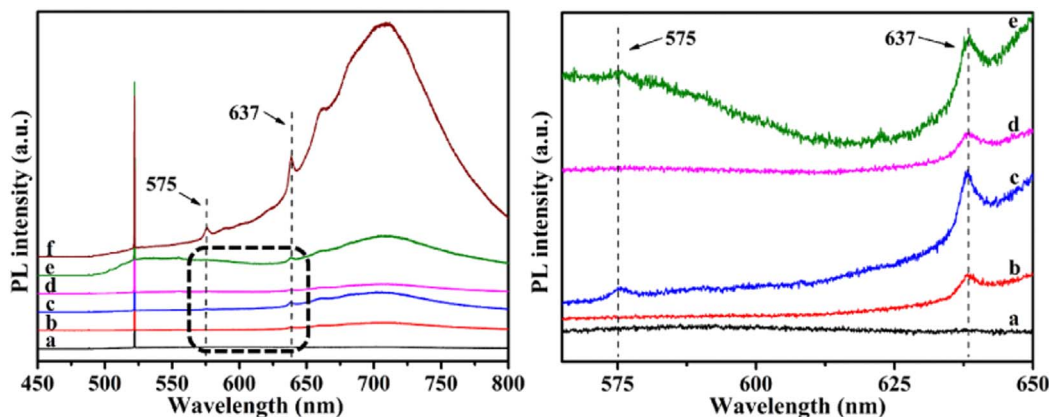


Fig. 7. PL spectra of the diamond crystals synthesized in the FeNi-S-C system; (a), (b), (c), (d), (e), and (f) are obtained in the E-1, E-2, E-3, E-4, E-5, and E-6 experiment, respectively.

References

- [1] B.M. Yan, X.P. Jia, C. Fang, N. Chen, Y.D. Li, S.S. Sun, H.A. Ma, The effect of phosphorus and nitrogen co-doped on the synthesis of diamond at high pressure and high temperature, *Int. J. Refract. Met. Hard Mater.* 54 (2016) 309–314.
- [2] L.F. Dobrzynetskaia, R. Wirth, H.W. Green, A look inside of diamond-forming media in deep subduction zones, *Proc. Natl. Acad. Sci. U. S. A.* 104 (2007) 9128–9132.
- [3] S. Masuya, K. Hanada, T. Oshima, H. Sumiya, M. Kasu, Formation of stacking fault and dislocation behavior during the high-temperature annealing of single-crystal HPHT diamond, *Diam. Relat. Mater.* 75 (2017) 155–160.
- [4] M.H. Hu, N. Bi, S.S. Li, T.C. Su, Q. Hu, X.P. Jia, H.A. Ma, Studies on synthesis and growth mechanism of high quality sheet cubic diamond crystals under high pressure and high temperature conditions, *Int. J. Refract. Met. Hard Mater.* 48 (2015) 61–64.
- [5] L. Zou, G.J. Dong, M. Zhou, Investigation on frictional wear of single crystal diamond against ferrous metals, *Int. J. Refract. Met. Hard Mater.* 41 (2013) 174–179.
- [6] E.I. Zhimulev, A.I. Chepurov, E.F. Sinyakova, V.M. Sonin, A.A. Chepurov, N.P. Pokhilenko, Diamond crystallization in the Fe-Co-S-C and Fe-Ni-S-C systems and the role of sulfide-metal melts in the genesis of diamond, *Geochem. Int.* 50 (2012) 205–216.
- [7] Y.N. Palyanov, Y.M. Borzdov, A.F. Khokhryakov, I.N. Kupriyanov, N.V. Sobolev, Sulfide melts–graphite interaction at HPHT conditions: implications for diamond genesis, *Earth Planet. Sci. Lett.* 250 (2006) 269–280.
- [8] J. Farquhar, B.A. Wing, K.D. Mckeegan, J.W. Harris, P. Cartigny, M.H. Thiemens, Mass-independent sulfur of inclusion in diamond and sulfur recycling on early earth, *Science* 298 (2002) 2369–2372.
- [9] E.M. Smith, S.B. Shirey, F. Nestola, E.S. Bullock, J.H. Wang, S.H. Richardson, W.Y. Wang, Large gem diamonds from metallic liquid in Earth's deep mantle, *Science* 354 (2016) 1403–1405.
- [10] Y.N. Palyanov, I.N. Kupriyanov, Y.M. Borzdov, A.G. Sokol, A.F. Khokhryakov, Diamond crystallization from a sulfur-carbon system at HPHT conditions, *Cryst. Growth Des.* 9 (2009) 2922–2926.
- [11] K. Sato, T. Katsura, Sulfur: a new solvent-catalyst for diamond synthesis under high-pressure and high-temperature conditions, *J. Cryst. Growth* 223 (2001) 189–194.
- [12] Y. Palyanov, Y. Borzdov, I. Kupriyanov, V. Gusev, A. Khokhryakov, A. Sokol, High-pressure synthesis and characterization of diamond from a sulfur-carbon system, *Diam. Relat. Mater.* 10 (2001) 2145–2152.
- [13] L. Zhou, X.P. Jia, H.A. Ma, L.X. Chen, W.L. Guo, Y.T. Li, Influences of additive sulfur on the synthesis of industrial diamonds, using Ni₇₀Mn₂₅Co₅ alloy powder as catalyst, *Diam. Relat. Mater.* 15 (2006) 1318–1322.
- [14] N. Chen, H.A. Ma, C. Fang, Y.D. Li, X.B. Liu, Z.X. Zhou, X.P. Jia, Synthesis and characterization of IIa-type S-doped diamond in FeNi catalyst under high pressure and high temperature conditions, *Int. J. Refract. Met. Hard Mater.* 66 (2017) 122–126.
- [15] Y. Li, X.P. Jia, H.A. Ma, J. Zhang, F.B. Wang, N. Chen, Y.G. Feng, Electrical properties of diamond single crystals co-doped with hydrogen and boron, *CrystEngComm* 16 (2014) 7547–7551.
- [16] L.Q. Ma, H.A. Ma, H.Y. Xiao, S.S. Li, Y. Li, X.P. Jia, Effect of additive boron on type-Ib gem diamond single crystals synthesized under HPHT, *Chin. Sci. Bull.* 55 (2010) 677–679.
- [17] A.S. Barnard, Diamond standard in diagnostics: nanodiamond biolabels make their mark, *Analyst* 1341 (2009) 1751–1764.
- [18] J.R. Maze, P. Cappellaro, L. Childress, M.V.G. Dutt, J.S. Hodges, S. Hong, L. Jiang, P.L. Stanwix, J.M. Taylor, E. Togan, A.S. Zibrov, P. Hemmer, A. Yacoby, R.L. Walsworth, M.D. Lukin, Nanoscale magnetic sensing using spin qubits in diamond, *Advanced Optical Concepts in Quantum Computing, Memory, and Communication II*, vol. 7225, 2009, pp. 1–8.
- [19] N. Mohan, C.S. Chen, H.H. Hsieh, Y.C. Wu, H.C. Chang, In vivo imaging and toxicity assessments of fluorescent nanodiamonds in *Caenorhabditis elegans*, *Nano Lett.* 10 (2010) 3692–3699.
- [20] P. Neumann, R. Kolesov, B. Naydenov, J. Beck, F. Rempp, M. Steiner, V. Jacques, G. Balasubramanian, M.L. Markham, D.J. Twitchen, S. Pezzagna, J. Meijer, J. Twamley, F. Jelezko, J. Wrachtrup, Scalable quantum register based on coupled electron spins in a room temperature solid, *Nat. Phys.* 6 (2010) 249–253.
- [21] Y.N. Palyanov, I.N. Kupriyanov, Y.M. Borzdov, A.F. Khokhryakov, N.V. Surovtsev, High-pressure synthesis and characterization of Ge-doped single crystal diamond, *Cryst. Growth Des.* 16 (2016) 3510–3518.
- [22] S. Schietinger, M. Barth, T. Aichele, O. Benson, Plasmon-enhanced single photon emission from a Nanoassembled metal-diamond hybrid structure at room temperature, *Nano Lett.* 9 (2009) 1694–1698.
- [23] J. Wrachtrup, F. Jelezko, Processing quantum information in diamond, *J. Phys. Condens. Matter* 18 (2006) S807–S824.
- [24] G. Davies, M.F. Hamer, Optical studies of the 1.945 eV Vibronic band in diamond, *Proc. R. Soc. Lond. A* 348 (1976) 285–298.
- [25] T. Gaebel, M. Domhan, C. Wittmann, I. Popa, F. Jelezko, J. Rabeau, et al., Photochromism in single nitrogen-vacancy defect in diamond, *Appl. Phys. B Lasers Opt.* 82 (2005) 243–246.
- [26] S. Pezzagna, D. Rogalla, D. Wildanger, J. Meijer, A. Zaitsev, Creation and nature of optical centres in diamond for single-photon emission—overview and critical remarks, *New J. Phys.* 13 (2011) 1–24.
- [27] A.R. Lang, M. Moore, A.P.W. Makepeace, W. Wierzbowski, C.M. Welbourn, On the dilatation of synthetic type Ib diamond by substitutional nitrogen impurity, *Phil. Trans. R. Soc. A* 337 (1991) 498–518.
- [28] K. Iakoubovskii, G.J. Adriaenssens, Trapping of vacancies by defects in diamond, *J. Phys. Condens. Matter* 13 (2001) 6015–6018.
- [29] L.B. Tsymbulov, L.S. Tsemekhman, Solubility of carbon in sulfide melts of the system Fe-Ni-S, *Russ. J. Appl. Chem.* 74 (2001) 925–929.
- [30] Z.Z. Liang, H. Kanda, X.P. Jia, H.A. Ma, P.W. Zhu, Q.F. Guan, C.Y. Zang, Synthesis of diamond with high nitrogen concentration from powder catalyst-C-additive NaN₃ by HPHT, *Carbon* 44 (2006) 913–917.
- [31] C. Fang, X.P. Jia, N. Chen, Y.D. Li, L.S. Guo, L.C. Chen, H.A. Ma, X.B. Liu, HPHT synthesis of N-H co-doped diamond single crystals, *J. Cryst. Growth* 436 (2016) 34–39.
- [32] M.H. Hu, N. Bi, S.S. Li, T.C. Su, Q. Hu, H.A. Ma, X.P. Jia, Synthesis and characterization of boron and nitrogen co-doped diamond crystals under high pressure and high temperature conditions, *CrystEngComm* 19 (2017) 4571–4575.
- [33] Z.Y. Wang, L.H. Dong, D.S. Wang, Y.H. Dong, Study of HPHT single crystal diamond as precision cutting tool material, *Precis. Eng.* 36 (2012) 162–167.
- [34] Y. Li, X.P. Jia, W. Shi, S.L. Leng, H.A. Ma, S.S. Sun, F.B. Wang, N. Chen, Y. Long, The preparation of new “BCN” diamond under higher pressure and higher temperature, *Int. J. Refract. Met. Hard Mater.* 43 (2014) 147–149.
- [35] K. Beha, A. Batalov, N.B. Manson, R. Bratschitsch, A. Leitenstorfer, Optimum photoluminescence excitation and recharging cycle of single nitrogen-vacancy centers in ultrapure diamond, *Phys. Rev. Lett.* 109 (2012) 1–5.
- [36] T.A. Kennedy, J.S. Colton, J.E. Butler, R.C. Linares, P.J. Doering, Long coherence times at 300 K for nitrogen-vacancy center spins in diamond grown by chemical vapor deposition, *Appl. Phys. Lett.* 83 (2003) 4190–4192.